Maintenance of Macrophage Redox Status by ChREBP Limits Inflammation and Apoptosis and Protects against Advanced Atherosclerotic Lesion Formation

Vincent Sarrazy, Sophie Sore, Manon Viaud, Guylène Rignol, Marit Westerterp, Franck Ceppo, Jean-François Tanti, Rodolphe Guinamard, Emmanuel L. Gautier, Laurent Yvan-Charvet

Article

Cell Reports

Maintenance of Macrophage Redox Status by ChREBP Limits Inflammation and Apoptosis and Protects against Advanced Atherosclerotic Lesion Formation

Graphical Abstract

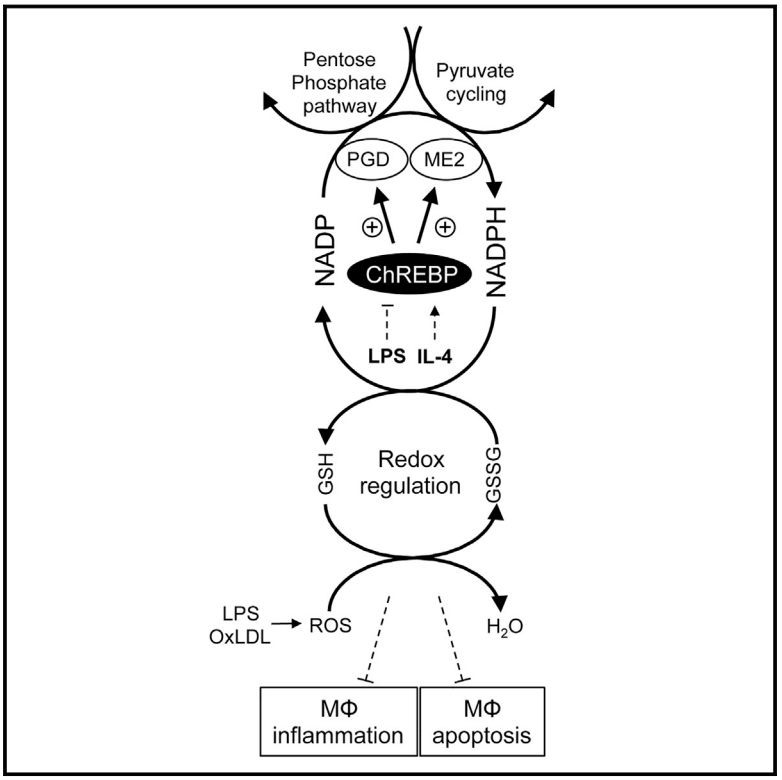

Authors

Vincent Sarrazy, Sophie Sore, Manon Viaud, ..., Rodolphe Guinamard, Emmanuel L. Gautier, Laurent Yvan-Charvet

Correspondence

laurent.yvan-charvet@unice.fr

In Brief

Sarrazy et al. show that the carbohydrate-responsive element binding protein ChREBP is required for metabolic reprogramming in activated macrophages and provide evidence that changes in ChREBP-dependent macrophage redox status influence macrophage polarization and survival with physiopathological consequences on atherosclerosis.

Highlights

- ChREBP prevents macrophage inflammatory responses and apoptosis
- ChREBP maintains macrophage redox status
- ChREBP protects against atherosclerosis development

Sarrazy et al., 2015, Cell Reports *13*, 132–144
October 6, 2015
http://dx.doi.org/10.1016/j.celrep.2015.08.068

OPEN ACCESS
CellPress

Cell Reports
Article

Maintenance of Macrophage Redox Status by ChREBP Limits Inflammation and Apoptosis and Protects against Advanced Atherosclerotic Lesion Formation

Vincent Sarrazy,[1] Sophie Sore,[1] Manon Viaud,[1] Guylène Rignol,[1] Marit Westerterp,[2] Franck Ceppo,[1] Jean-Francois Tanti,[1] Rodolphe Guinamard,[1] Emmanuel L. Gautier,[3] and Laurent Yvan-Charvet[1,*]

[1]Institut National de la Santé et de la Recherche Médicale (INSERM) U1065, Centre Méditerranéen de Médecine Moléculaire (C3M), Atip-Avenir, 06204 Nice, France

[2]Division of Molecular Medicine, Department of Medicine, Columbia University, New York, NY 10032, USA

[3]Institut National de la Santé et de la Recherche Médicale (INSERM) UMR_S 1166, Pierre and Marie Curie University Paris 6, ICAN Institute of Cardiometabolism and Nutrition, 75006 Paris, France

*Correspondence: laurent.yvan-charvet@unice.fr

http://dx.doi.org/10.1016/j.celrep.2015.08.068

SUMMARY

Enhanced glucose utilization can be visualized in atherosclerotic lesions and may reflect a high glycolytic rate in lesional macrophages, but its causative role in plaque progression remains unclear. We observe that the activity of the carbohydrate-responsive element binding protein ChREBP is rapidly downregulated upon TLR4 activation in macrophages. ChREBP inactivation refocuses cellular metabolism to a high redox state favoring enhanced inflammatory responses after TLR4 activation and increased cell death after TLR4 activation or oxidized LDL loading. Targeted deletion of ChREBP in bone marrow cells resulted in accelerated atherosclerosis progression in *Ldlr*$^{-/-}$ mice with increased monocytosis, lesional macrophage accumulation, and plaque necrosis. Thus, ChREBP-dependent macrophage metabolic reprogramming hinders plaque progression and establishes a causative role for leukocyte glucose metabolism in atherosclerosis.

INTRODUCTION

Atherosclerosis is a chronic inflammatory disease driven by the accumulation of macrophage foam cells in the artery walls (Ross, 1999; Hansson et al., 2006; Moore and Tabas, 2011). Circulating monocytes traverse the inflamed arterial endothelium to fuel developing lesions (Swirski and Nahrendorf, 2013; Zernecke and Weber, 2014; Randolph, 2014; Tall and Yvan-Charvet, 2015). In addition, local environmental cues lead to alterations in the phenotype and survival of lesional macrophages (Tabas, 2005; Mosser and Edwards, 2008; Van Vré et al., 2012; Chinetti-Gbaguidi and Staels, 2011; Hasty and Yvan-Charvet, 2013), altering plaque composition and increasing the vulnerability of the plaques to rupture (Libby et al., 1996; Kolodgie et al., 2004).

Although extensive research has focused on elucidating the roles of cytokines and the microenvironment in the migration, proliferation, differentiation, and apoptosis of monocytes and macrophages, the cellular metabolic pathways that regulate these processes are not well understood. Inflamed atherosclerotic plaques can be visualized by non-invasive positron emission tomography-computed tomography (PET-CT) imaging with ^{18}FDG, a glucose analog, which correlates with macrophage accumulation and inflammation (Rogers and Tawakol, 2011; Garcia-Garcia et al., 2014). Increasing glucose metabolism is thought to be crucial for macrophage activation. For instance, glucose consumption and glycolysis are enhanced in macrophages during inflammatory responses (Fukuzumi et al., 1996; Gamelli et al., 1996), and pharmacological inhibition of glucose metabolism can prevent the inflammatory responses induced by lipopolysaccharide (LPS) (Gautier et al., 2013). However, a recent study has called into question the relevance of these observations, as myeloid-specific overexpression of the glucose transporter Glut1, achieved by transducing bone marrow (BM) with CD68-Glut1 retroviral particles, did not aggravate atherosclerosis in *Ldlr*$^{-/-}$ knockout mice compared to Glut1-sufficient controls despite enhanced macrophage glycolysis (Nishizawa et al., 2014). Thus, there is a need for a better understanding of the metabolic pathways that link macrophage cellular glucose homeostasis and inflammation in atherosclerosis.

There are a number of pathways leading to aberrant metabolism of glucose that are thought to be pathological. Studies in mice have shown that glucose can be reduced by aldose reductase (AR) to sorbitol in macrophages, leading to the production of excess reactive oxygen species (ROS), which may contribute to accelerated atherosclerosis (Srivastava et al., 2009; Vedantham et al., 2011; Vikramadithyan et al., 2005). However, low levels of AR are present in mice, and this pathway has few effects in mouse macrophages unless they express a human AR transgene, suggesting that alternative metabolic pathways exist to drive the inflammatory responses observed during macrophage activation. Modulation of mitochondrial potential and the tricarboxylic (TCA) cycle has been clearly associated with the ability of macrophages to mount an inflammatory

response (Vats et al., 2006; O'Neill and Hardie, 2013; Tannahill et al., 2013; Jha et al., 2015). Recently, the sedoheptulose kinase CARKL, an enzyme involved in the pentose phosphate pathway (PPP), has been proposed to act upstream of these alterations by modulating glycolysis, oxidative phosphorylation (OXPHOS), and the TCA cycle in macrophages, with subsequent modulation of inflammatory responses (Haschemi et al., 2012). Intriguingly, the carbohydrate-responsive element-binding protein (ChREBP), also known as MLX-interacting protein-like (MLXIPL), is a glucose-responsive transcription factor that regulates glycolysis and lipogenesis in hepatocytes. ChREBP can also be either positively regulated by glucose-derived metabolites or negatively regulated by AMPK and PKA, illustrating its pivotal role at the interface of different metabolic pathways (Filhoulaud et al., 2013). However, the relevance of this pathway to macrophage activation and atherosclerosis remains unknown.

To test the causal relationship between modulation of myeloid glucose utilization, inflammatory activation of myeloid cells, and the development of atherosclerotic lesions, we examined the role of ChREBP in inflammatory macrophages. We found that ChREBP activity was downregulated upon LPS stimulation, and knockdown of ChREBP in macrophages led to a major defect in the metabolic pathways that generate NADPH, the rate-limiting source of reduced glutathione. This led to increased inflammatory cytokine production and increased apoptosis in response to both LPS and oxidized LDL after ChREBP knockdown in macrophages. We next transplanted the BM of mice with ChREBP deficiency into atheroprone *Ldlr*$^{-/-}$ mice. Unexpectedly, we found that *Ldlr*$^{-/-}$ mice that had received *Chrebp*$^{-/-}$ BM showed accelerated atherosclerosis, with macrophage accumulation and enhanced necrotic core formation. These data demonstrate an important anti-inflammatory and pro-survival role for ChREBP in the prevention of atherosclerosis and necrotic core formation.

RESULTS

ChREBP Deficiency Increases Expression of Inflammatory Cytokines in Macrophages

Given the enhanced glucose flux observed in inflammatory macrophages (Fukuzumi et al., 1996; Gamelli et al., 1996; Gautier et al., 2013; Nishizawa et al., 2014), we first investigated whether the activity of ChREBP, a glucose-responsive transcriptional factor, was enhanced upon LPS stimulation in thioglycollate-elicited peritoneal macrophages. Surprisingly, ChREBP nuclear translocation, reflecting ChREBP activity, was reduced by ~2-fold after 3 hr of LPS stimulation in wild-type (WT) macrophages (Figures 1A and 1B). In an attempt to identify the underlying mechanism, we next tested whether reduced CARKL-dependent X5P production upon macrophage activation (Haschemi et al., 2012) could prevent ChREBP nuclear translocation and activity (Filhoulaud et al., 2013). Intriguingly, CARKL silencing using small interfering RNA (siRNA) reduced ChREBP nuclear translocation both at baseline and after LPS stimulation, but this most likely reflected reduced total ChREBP protein expression (Figure S1). Mechanistic studies were next carried out using siRNA that led to a significant decrease in ChREBP mRNA expression (Figure S2A). ChREBP protein expression and nuclear translocation confirmed the knockdown efficiency (Figures 1A and 1B). A time-course experiment showed a greater initial increase in the expression of genes encoding cytokines such as tumor necrosis factor α (TNF-α) and interleukin-6 (IL-6) in macrophages after ChREBP silencing, which returned to basal levels after 10 hr of LPS exposure (Figures 1C and 1D). A 2-fold increase in TNF-α and IL-1β secretion paralleled the mRNA response 3 hr after LPS challenge (Figure 1E). These data, together with enhanced surface staining of the co-stimulatory molecule CD80 upon LPS stimulation in ChREBP knockdown macrophages (Figure 1F), demonstrated an enhanced activation state of these cells. LPS is known to signal via the Toll-like receptor 4 (TLR4)/nuclear factor κB (NF-κB) pathway, and ChREBP knockdown resulted in a greater initial increase and sustained phosphorylation in the transactivation domain of the p65 subunit, which is essential for optimal NF-κB activation after LPS exposure (Figure 1G). An alkaline phosphatase reporter construct inducible by NF-κB in RAW-Blue cells confirmed an increase in NF-κB transcriptional activity after ChREBP silencing from 3 hr to 6 hr after LPS stimulation (Figure 1H). This appears to be specific to the NF-κB pathway, as similar phosphorylation of Akt, p38-MAPK, and mTor was observed after ChREBP knockdown in macrophages 3 hr after LPS treatment (Figure S2B). We finally evaluated cytokine gene expression BM-derived macrophages. Although there was no detectable basal expression of cytokines in either controls or ChREBP knockdown macrophages, an enhanced response to LPS was confirmed in ChREBP knockdown BM-derived macrophages (Figure S2C). Thus, ChREBP downregulation after LPS stimulation affects the inflammatory response in macrophages.

Metabolic Profiling Reveals Reduced Metabolic Pathways that Control NADPH Production in LPS-Stimulated *Chrebp*-Deficient Macrophages, Favoring Catabolic over Anabolic Pathways

Considering the substantial reprogramming of metabolism upon macrophage activation, we next quantified glycolytic metabolites by liquid chromatography-mass spectrometry in thioglycollate-elicited peritoneal macrophages after ChREBP knockdown with or without 3 hr LPS treatment. Unexpectedly, despite the role of ChREBP as a positive regulator of glycolysis in hepatocytes (Dentin et al., 2012), increases in glycolytic metabolites such as fructose 1,6-biphosphate (FBP) and 3-phosphoglycerate/2-phosphoglycerate (3PG+2PG) were observed in basal ChREBP knockdown macrophages even thought these effects were not sustained upon LPS stimulation (Figure 2A). Glucose 6-phosphate/fructose 6-phosphate (G6P+F6P) and citric acid cycle metabolites such as citrate/isocitrate (I/Citrate) and succinate were not statically different in macrophages following ChREBP silencing (Figures 2A and 2B). In contrast, a striking increase in malate (more than 3-fold) was observed in basal and LPS-stimulated ChREBP knockdown macrophages (Figure 2B). This was associated with a trend toward a higher ATP-to-ADP ratio in basal ChREBP knockdown macrophages (Figure 2C, left panel) and an ~1.6-fold increase in lactate content (a surrogate of glycolytic flux) in basal and LPS-stimulated ChREBP knockdown macrophages (Figure 2C, right panel). The metabolic plasticity of ChREBP-deficient macrophages

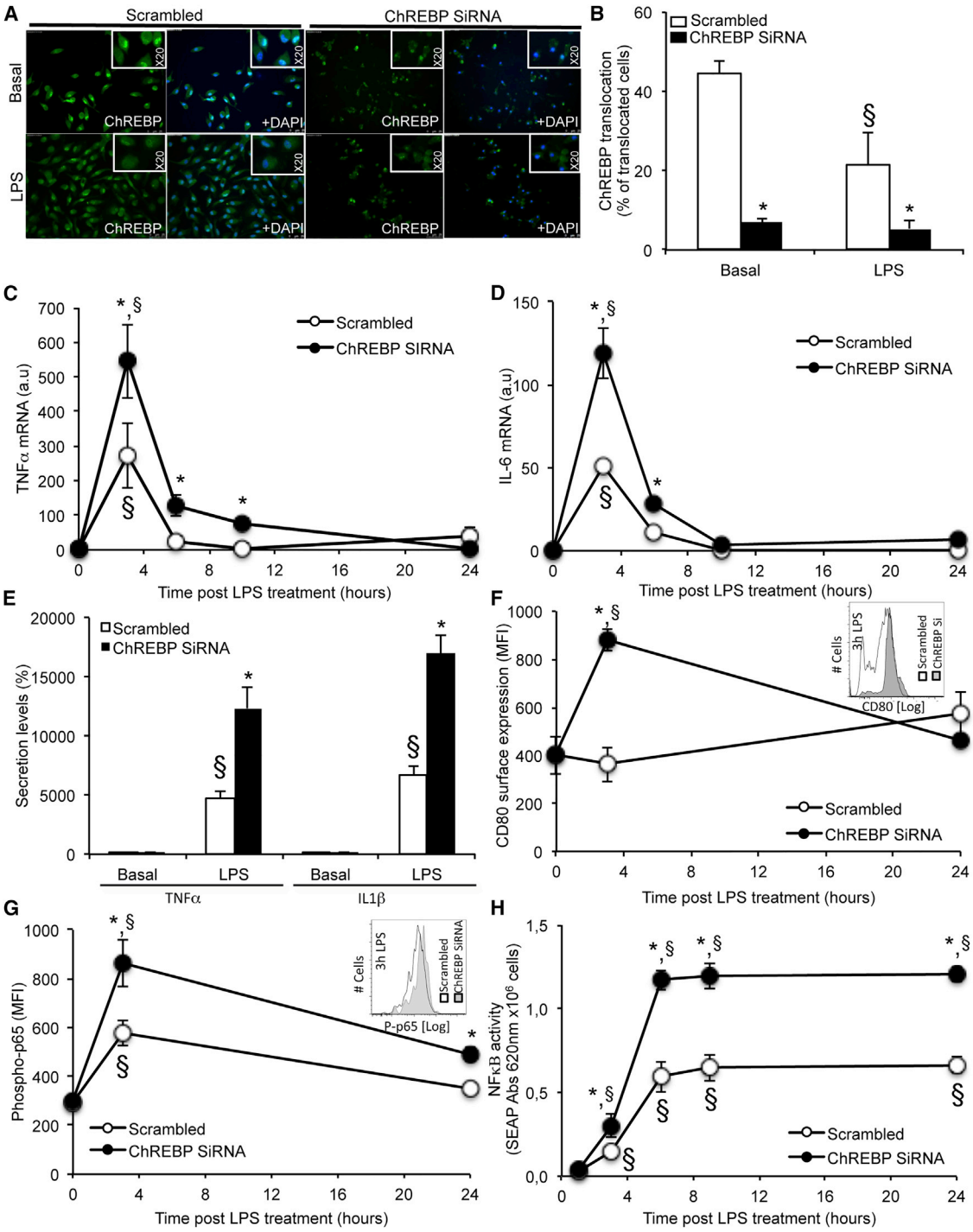

Figure 1. ChREBP Is Required for the Proper Inflammatory Response of Macrophages

Thioglycollate-elicited peritoneal macrophages transfected for 48 hr with scrambled or ChREBP siRNA were stimulated with or without 100 ng/ml LPS for 3 hr or the indicated period of time.

(A and B) Representative pictures and quantification of ChREBP translocation (magnification 5×, insert 20× with or without DAPI co-staining).

(C and D) mRNA expression over time of TNF-α and IL-6.

(E) Secretion of inflammatory cytokines normalized to cellular protein amount and expressed as a percentage of WT.

(F and G) CD80 surface expression (F) and phospho-p65 expression (G) over time.

(H) NF-κB activity measured by an alkaline phosphatase reporter construct in RAW-Blue cells.

Values are mean ± SEM of three independent experiments. *p < 0.05 compared to control; §p < 0.05 versus untreated condition.

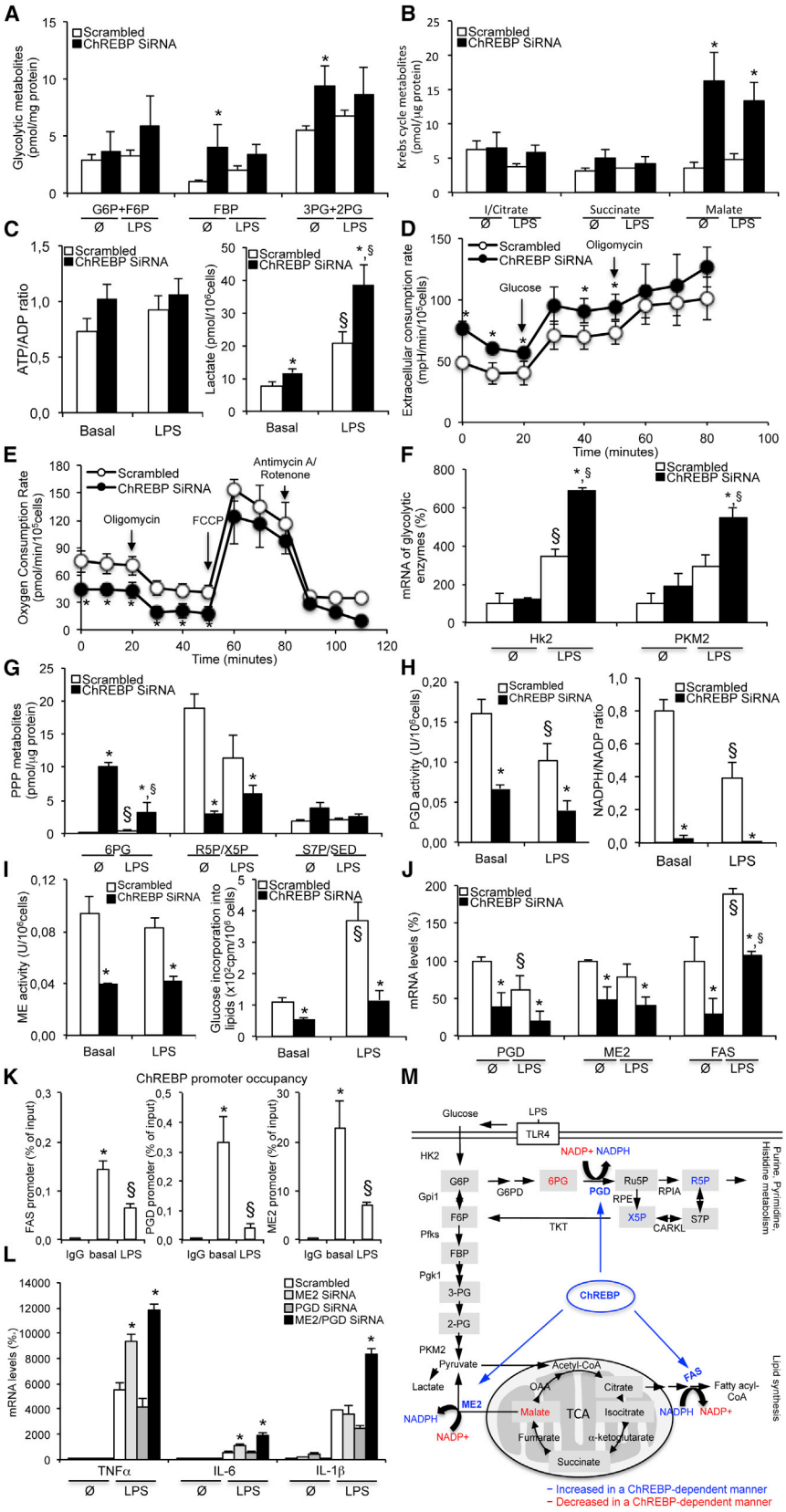

Figure 2. ChREBP Reprograms Carbohydrate Metabolism in LPS-Stimulated Macrophages

Thioglycollate-elicited peritoneal macrophages transfected with scrambled or ChREBP siRNA were stimulated with or without 100 ng/ml LPS for 3 hr or the indicated period of time.

(A–C) Effect of LPS treatment on glycolytic (A) and citric acid (B) metabolites and ATP/ADP ratio and lactate (C).

(D and E) ECAR (D) and OCR (E) recordings of 3-hr LPS-stimulated macrophages under the indicated conditions.

(F–J) Effect of LPS treatment on mRNA expression of glycolytic enzymes (F), metabolites from the pentose phosphate pathway (G), PGD activity and NADPH/NAD ratio (H), ME activity and glucose conversion into lipids (I), and mRNA expression of NADPH-dependent enzymes (J).

(K) ChIP assays were performed with amplicons flanking the proximal promoter region of putative ChREBP targets. qPCR (normalized to input) was used to assess ChREBP occupancy of the targeted promoter.

(L) Effect of LPS on cytokine gene expression in macrophages transfected with scrambled, ME2, and PDG siRNA.

Results are means ± SEM of an experiment performed in triplicate. *$p < 0.05$ compared to control; §$p < 0.05$ versus untreated condition.

(M) Schematic representation of the metabolic pathways regulated by ChREBP in LPS-treated macrophages.

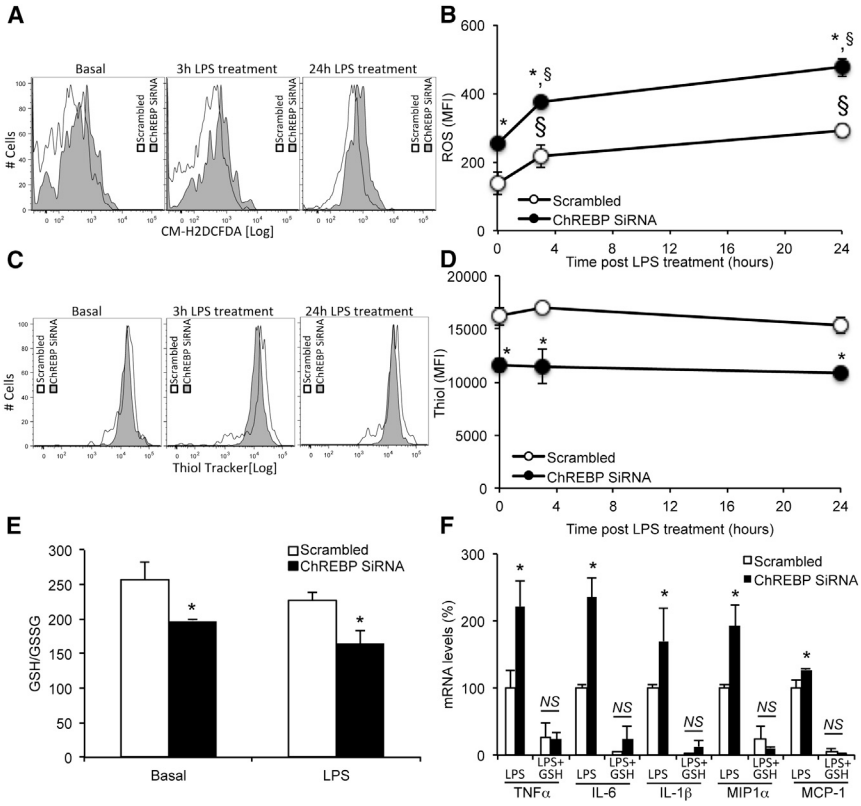

Figure 3. The Enhanced Inflammatory Response in *Chrebp*-Deficient Macrophages Is Metabolically Driven by Low Glutathione Redox Status

Thioglycollate-elicited peritoneal macrophages transfected with scrambled or ChREBP siRNA were stimulated with or without 100 ng/ml LPS for 3 hr or the indicated period of time.

(A–D) Representative histograms and quantification of ROS generation (A and B) and intracellular thiol content (C and D).

(E) Intracellular GSH/GSSG ratio.

(F) Effect of GSH on transcript levels of inflammatory cytokines (percentage over WT).

Results are means ± SEM of three independent experiments. *p < 0.05 compared to control; §p < 0.05 versus untreated condition.

upon activation was also confirmed by an increase in extracellular acidification rate (ECAR) at baseline and after glucose stimulation, but not after oligomycin treatment (Figure 2D), and a decrease in oxygen consumption rate (OCR) at baseline or after oligomycin treatment (Figure 2E). An ~2-fold increase in the expression of glycolytic enzymes such as hexokinase 2 (Hk2) and pyruvate kinase isozyme M2 (PKM2) in LPS-stimulated macrophages after ChREBP knockdown also correlated with higher glycolytic flux (Figure 2F). Although increased 6-phosphogluconate (6PG) was observed in basal and LPS-stimulated macrophages after ChREBP silencing, there was a significant decrease in ribulose-5-phosphate/xybulose-5-phosphate (R5P/X5P) levels, but not sedoheptulose-7phosphate/sedoheptulose (S7P/SED), in these cells (Figure 2G). This was associated with an ~2-fold decrease in phosphogluconate dehydrogenase (PGD; an enzyme that converts 6PG into R5P and NADP+ to NADPH) activity in basal and LPS-stimulated ChREBP knockdown cells (Figure 2H, left panel). Consistently, basal and LPS-stimulated macrophages exhibited a prominent 30-fold decrease in the NADPH/NADP ratio after ChREBP knockdown (Figure 2H, right panel). NADPH can also be produced by the pyruvate cycling pathway or consumed through anabolic pathways such as lipid synthesis, both pathways being targets of ChREBP (Ma et al., 2006; Burgess et al., 2008; Filhoulaud et al., 2013). Remarkably, we found a 2.5-fold decrease in malic enzyme (ME) activity (Figure 2I, right panel) and a 2-fold decrease in glucose conversion into lipids (Figure 2I, left panel) in basal and LPS-stimulated macrophages after ChREBP knockdown. At the transcriptional level, an ~2-fold decrease in phosphogluconate dehydrogenase (PGD), mitochondrial malic enzyme (ME2), and fatty acid synthase (FAS) mRNA expression was observed in basal and LPS-stimulated macrophages after ChREBP silencing (Figure 2J), and this correlated with an altered NADPH/NAPD ratio and impaired lipid synthesis. Then, specific binding of ChREBP on FAS, ME2, and PGD promoters was investigated in basal and LPS-stimulated macrophages using chromatin immunoprecipitation assays. The binding of ChREBP was demonstrated at different degrees on these promoters and declined after 3-hr LPS stimulation (Figure 2K). ME2 and PGD silencing using siRNA in thioglycollate-elicited peritoneal macrophages with or without 3-hr LPS treatment also confirmed that combined knockdown of these two genes led to an exacerbated inflammatory response after LPS stimulation (Figure 2L). Together, our results reveal that ChREBP does not contribute to the enhanced glycolysis in inflamed macrophages but rather controls the two main cellular pathways involved in NAPDH production, which could explain, together with reduced FAS expression, the diminished lipid synthesis capacity of these cells (Figure 2M).

Reduced PPP-Dependent Cellular Redox Status Drives the Macrophage Inflammatory Response in *Chrebp*-Deficient Macrophages

In metabolic terms, the reduced NADPH/NADP ratio observed in macrophages after ChREBP silencing could equate to a lack of reducing energy known to supply reduced glutathione and scavenge free radicals to prevent oxidative damage. Indeed, a time-course experiment revealed that ChREBP knockdown in thioglycollate-elicited peritoneal macrophages led to an ~1.7-fold increase in the oxidative stress response measured by flow cytometry (Figures 3A and 3B) that was inversely correlated with an ~1.4-fold decrease in thiol-tracker staining under basal or LPS-stimulated conditions (Figures 3C and 3D). Increased oxidative stress response was also observed to a less extent in

thioglycollate-elicited peritoneal macrophages cultured in low-glucose medium (5.6 mM versus 25 mM) after ChREBP silencing (Figure S3). The reduced GSH/GSSG balance in basal (1.3-fold) and LPS-stimulated (1.4-fold) macrophages after ChREBP knockdown confirmed an alteration of the glutathione redox balance in these cells (Figure 3E). Remarkably, exogenous addition of glutathione monoethyl ester clearly abolished the increased inflammatory cytokine expression induced by LPS in thioglycollate-elicited peritoneal macrophages after ChREBP silencing (Figure 3F). Together, these findings show that the increased inflammatory responses in macrophages with ChREBP silencing reflect a lack of NADPH-dependent reduction of glutathione disulfide.

Reduced M2 Polarization in *Chrebp*-Deficient Macrophages

As the modulation of the redox status alters macrophage M2 polarization (Vats et al., 2006; Haschemi et al., 2012; Jais et al., 2014), we next investigated the relevance of ChREBP in this pathway. Nuclear translocation of ChREBP was increased by almost 2-fold after IL-4 stimulation in thioglycollate-elicited peritoneal macrophages (Figures S4A and S4B). A time-course experiment showed that ChREBP silencing partially prevented the initial increase in Arg1 and Mrc1 mRNA expression induced by IL-4 (Figures S4C and S4D). Interestingly, treatment of IL-4-stimulated ChREBP knockdown macrophages with the antioxidant glutathione restored Arg1, Mrc1, and Fizz1 mRNA expression to the level of control cells, suggesting that ChREBP acts at the interface between macrophage M1-M2 polarization by controlling the redox status of the cells and most likely "pre-programming" macrophage skewing (Figure S4E) (Jais et al., 2014). As autophagy controls the delivery of lipids to lysosomes for hydrolysis (Ouimet et al., 2011) and lysosomal lipolysis has recently emerged as critical for M2 activation (Huang et al., 2014), we next wondered whether the altered fatty acid homeostasis in macrophages after ChREBP knockdown could modulate this pathway. ChREBP silencing prevented the rise in autophagic flux induced by IL-4 as quantified by flow cytometry (Figure S4F). Moreover, inhibition of autophagy by 3-methyladenine (3-MA) reduced the polarization of M2 macrophages induced by IL-4 in control macrophages to the same extent as that in ChREBP knockdown macrophages, as measured by Arg1, Mrc1, and Fizz1 mRNA expression (Figure S4E). Together, these findings suggest that ChREBP controls autophagy-dependent M2 polarization by maintaining macrophage redox status and fatty acid production.

Increased Susceptibility of *Chrebp*-Deficient Macrophages to Cell Death Induced by LPS and Oxidized LDL-Dependent ROS Generation

To test whether the reduced redox state of macrophages after ChREBP silencing contributes to an increased susceptibility to oxidative stress-induced apoptosis, thioglycollate-elicited peritoneal macrophages were treated with 100 ng/ml LPS or 50 μg/ml oxidized LDL for 24 hr. As expected, flow cytometry analysis revealed that WT macrophages were alive 24 hr after treatment (Figures 4A and 4B), whereas ChREBP knockdown macrophages showed a dramatic 4-fold increase in macrophage death, reflected by late apoptosis or necrosis (i.e., AnnexinV+ PI+) (Figures 4A and 4B). While reduced cellular thiols were present in viable, apoptotic, and necrotic macrophages after ChREBP knockdown in all the treatment groups (Figure 4C), the increase in ROS formation was mainly attributable to cells undergoing apoptosis and necrosis (Figure 4D). Because LPS and oxidized LDL-induced ROS production can promote caspase-dependent cell death in macrophage foam cells (Yvan-Charvet et al., 2010a), and recent data have shown an intimate link between glucose metabolism and caspase activation in experimental model of apoptosis induced by staurosporine (Pradelli et al., 2014), we next measured caspase activity. Flow cytometry analysis of fluorescent label carboxyfluorescein (FAM) fluorescent-labeled inhibitor of caspases (FICA) revealed an increase in caspase activity in apoptotic and necrotic ChREBP knockdown macrophages upon LPS or oxidized LDL stimulation compared to controls (Figures 4E and 4F). The addition of glutathione or pharmacological inhibition of caspases by Z-VAD-FMK confirmed marked antiapoptotic effects in oxidized LDL-stimulated *Chrebp*-deficient macrophages (Figure 4G). Together, these findings reveal a role of ChrREBP in maintaining macrophage redox status to limit caspase-dependent death.

Accelerated Atherosclerosis in *Ldlr*$^{-/-}$ Mice Transplanted with *Chrebp*$^{-/-}$ BM

Atherosclerosis is a chronic inflammatory disease dominated by a phenotypic switch of macrophages (Hasty and Yvan-Charvet, 2013) and alteration of macrophage survival (Tabas, 2005; Van Vré et al., 2012). We wondered whether expression of ChREBP by macrophages might affect atherosclerosis development. To test this hypothesis, we transplanted BM cells from WT and *Chrebp*$^{-/-}$ mice into irradiated *Ldlr*$^{-/-}$ recipients, thereby generating *Ldlr*$^{-/-}$ mice with either *Chrebp*$^{-/-}$ or WT macrophages. Four weeks after transplantation, mice were challenged with a Western-type diet for 11 weeks. Freshly isolated resident peritoneal macrophages at the end of the experiment showed no detectable ChREBP mRNA expression. TNF-α expression was increased by 2.5-fold and that of MCP-1 by 1.6-fold (Figure 5A), similar to the enhanced TNF-α and MCP-1 mRNA expression observed in LPS-stimulated *Chrebp*$^{-/-}$ thioglycollate-elicited peritoneal macrophages isolated from chow-fed animals compared to controls (Figure S5). This confirmed the efficiency of the transplantation procedure. Lipoprotein and metabolic parameters were measured before the start of the diet and at the time of sacrifice. As shown in Table S2, the two groups of mice did not differ significantly with regards to body weight, fat mass, plasma leptin, glucose and triglyceride levels, or plasma LDL and HDL cholesterol. We also did not observe changes in blood leukocytes, lymphocytes or spleen weight in *Chrebp*$^{-/-}$ BM transplanted mice before the start or at the end of the experiment (Table S2). A role of ChREBP in mediating glycolysis-induced T cell activation (Macintyre et al., 2014) was also excluded in *Chrebp*$^{-/-}$ BM recipients, as a similar percentage of CD44^{hi}CD62L^{lo} peripheral CD4^{+} and CD8^{+} lymphocytes was observed at sacrifice (Figure S6). Nevertheless, *Ldlr*$^{-/-}$ mice receiving *Chrebp*$^{-/-}$ BM showed an ~1.7-fold increase in atherosclerosis development

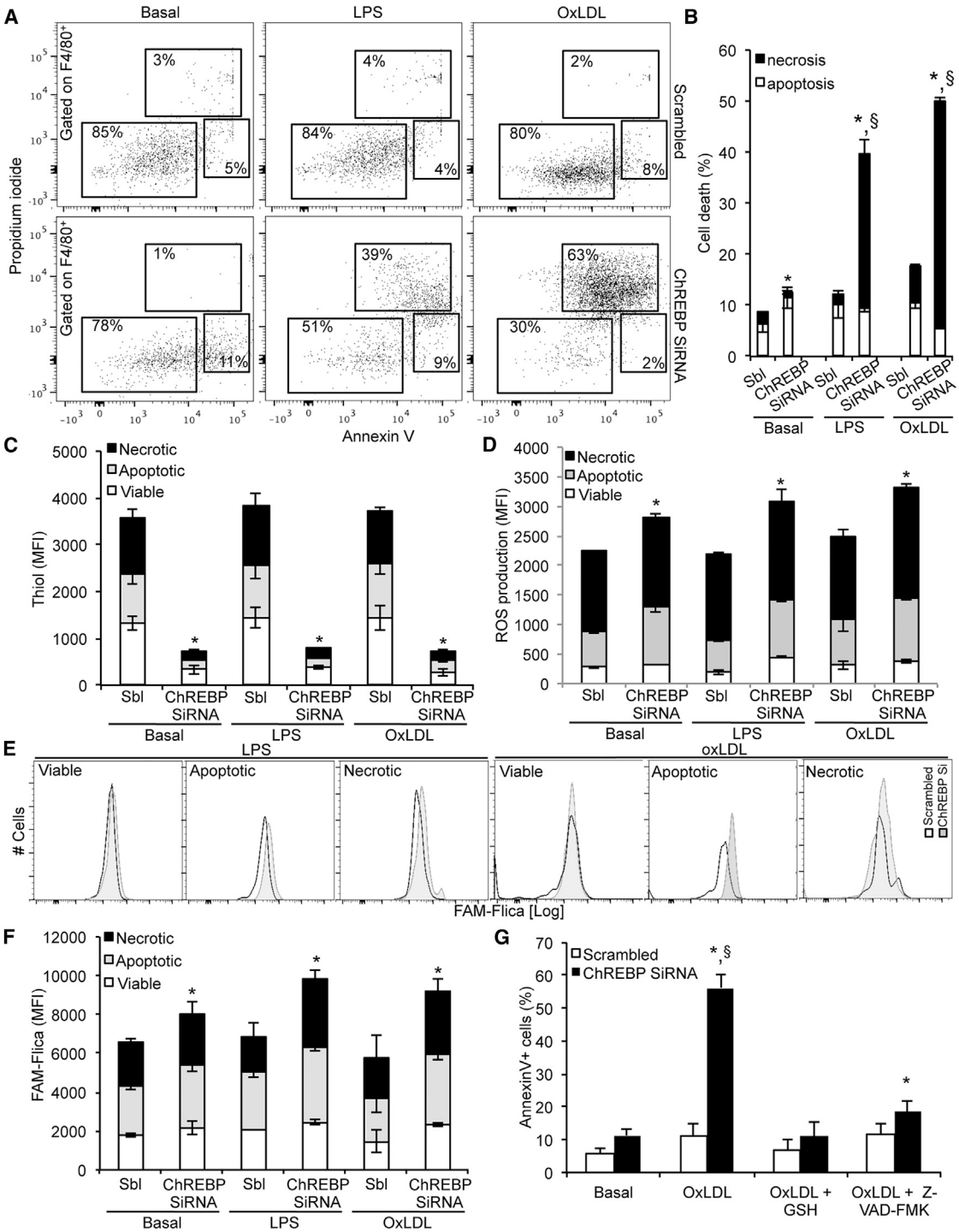

Figure 4. Enhanced Susceptibility to Cell Death in *Chrebp*-Deficient Macrophages Macrophages

(A and B) Representative FACS plots (A) and quantification of macrophage death (B) in thioglycollate-elicited peritoneal macrophages transfected with scrambled or ChREBP siRNA and treated with 100 ng/ml LPS or 50 μg/ml oxidized LDL (oxLDL) for 16 hr.

(C and D) Thiols (C) and ROS repartition (D) in necrotic, apoptotic, and viable cells.

(E and F) Representative histograms (E) and quantification (F) of caspase activation.

(G) Effect of GSH and Z-VAD-FMK caspase inhibitor on the percentage of Annexin V+ cells after 16-hr treatment with 50 μg/ml oxLDL.

Values are mean ± SEM. *p < 0.05 compared to control.

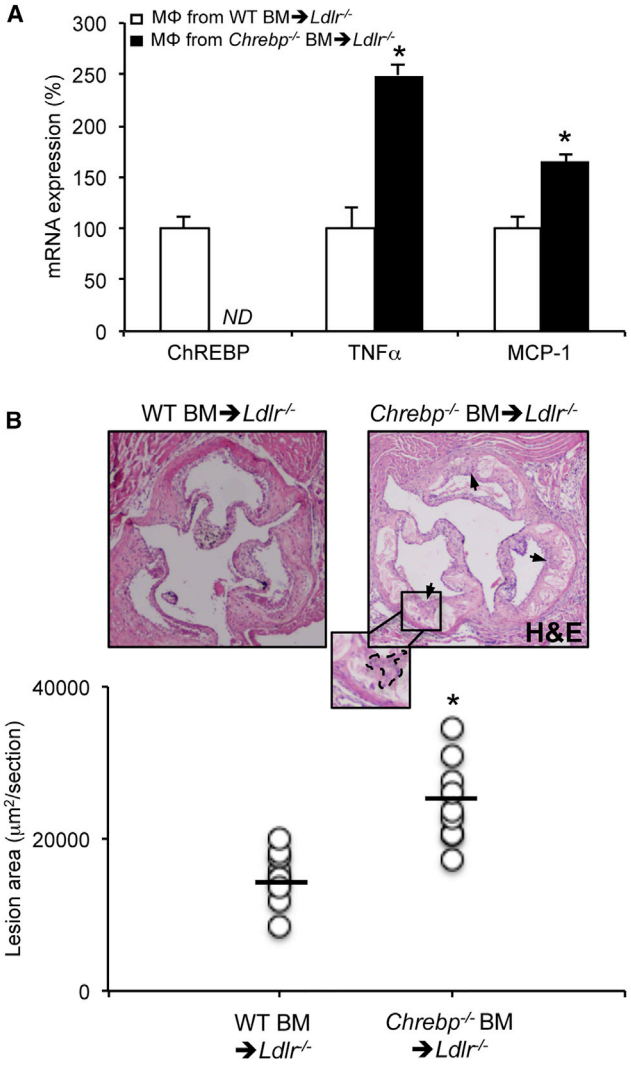

Figure 5. ChREBP Deficiency Promotes Accelerated Atherosclerosis

(A) mRNA levels in resident peritoneal macrophages isolated from high-fat diet (HFD)-fed *Ldlr*$^{-/-}$ recipient mice transplanted with WT or *Chrebp*$^{-/-}$ BM. (B) Representative H&E staining (magnification 100×, insert 200×) and quantification of atherosclerotic lesion development in the proximal aorta of HFD-fed *Ldlr*$^{-/-}$ mice transplanted with WT or *Chrebp*$^{-/-}$ BM (n = 10). Arrows and dashed lines depict inflammatory infiltrates.

in their proximal aortas and showed numerous inflammatory infiltrates compared to mice receiving WT BM, which developed only sparse foam cell-containing atherosclerotic lesions (Figure 5B).

Monocytosis in *Chrebp*$^{-/-}$ BM-Transplanted *Ldlr*$^{-/-}$ Mice Is Mediated through a Cell-Extrinsic Mechanism

Immunohistochemical staining of aortic root plaques confirmed a 2-fold increase in F4/80^{+} macrophages in *Chrebp*$^{-/-}$ BM-transplanted *Ldlr*$^{-/-}$ mice (Figure 6A). The increased plaque macrophage content in *Chrebp*$^{-/-}$ atheromata could reflect local inflammation or systemic monocytosis, which are known to contribute to atherosclerotic plaque progression in both mice and humans (Coller, 2005; Swirski et al., 2007; Tacke et al., 2007; Combadière et al., 2008). We observed a 2-fold increase in neutrophils and inflammatory blood Ly6C^{hi} monocyte subsets in *Chrebp*$^{-/-}$ BM-transplanted *Ldlr*$^{-/-}$ mice fed a high-fat diet (Figure 6B). We next undertook studies to elucidate the mechanisms underlying the peripheral inflammatory phenotype observed in these mice. Targeted gene expression profiling revealed that ChREBP was barely detectable in BM progenitors compared to macrophages (Figure S7A), even though ChREBP expression in these cells was much lower than in hepatocytes (Figure S7B). Gavage with a liver X receptor (LXR) agonist (TO-901317) that has been previously suggested to increase ChREBP expression in hepatocytes (Cha and Repa, 2007; Denechaud et al., 2008) did not modulate macrophage ChREBP expression (Figure S7A). ChREBP was also barely expressed in splenic dendritic cells or B and T lymphocytes compared to macrophages (Figure S7C). Taking advantage of a publically available gene expression dataset from Immgen (http://www.immgen.org), we observed that key enzymes of the PPP were predominantly expressed in cells derived from the macrophage lineage (Figure S7D), paralleling ChREBP expression. This further illustrated an important unrecognized role of this pathway in macrophages. Consistent with these findings, neither the Lin^{-}Sca1^{+}cKit^{+} (LSK) population, representing hematopoietic stem and progenitor cells (HSPCs), nor the granulocyte-monocyte progenitor (GMP) and common myeloid progenitor (CMP) populations were altered in the BM of mice transplanted with *Chrebp*$^{-/-}$ BM (Figure 6C). Nevertheless, monocyte counts were reduced in the BM of mice that had received *Chrebp*$^{-/-}$ BM, and this contrasted with the increase in Ly6C^{hi} monocytes observed in their spleen, most likely reflecting monocyte mobilization (Figures 2C and 2D). Measurement of various plasma factors known to promote BM hematopoietic cell mobilization did not reveal an alteration in growth factors such as GH, M-CSF or G-CSF (Figure S7E) or chemoattractant molecules such as MIP1α, MIP2, or KC (Figure S7F) in mice transplanted with *Chrebp*$^{-/-}$ BM. However, there was a significant 1.5-fold increase in levels of plasma MCP-1 and MCP-3, but not MCP-5, in these mice (Figure 6E). These chemokines have been previously been shown to be produced by macrophage foam cells (Westerterp et al., 2013) and to promote CCR2-dependent monocyte mobilization from the BM to the blood (Tsou et al., 2007). Thus, we wondered whether the monocytosis observed upon myeloid ChREBP deficiency could be dependent on systemic inflammation driven by macrophages. To directly test our hypothesis, we performed a competitive BM transplantation. *Ldlr*$^{-/-}$ mice were transplanted with a 1:1 mix of CD45.1 WT with either CD45.2 WT or CD45.2 *Chrebp*$^{-/-}$ BM. Mice were fed a high fat diet, and monocyte levels were assessed. In line with our previous observations, more CD45.2 Ly6C^{hi} monocytes were observed in mice containing *Chrebp*$^{-/-}$ cells (Figure 6F). Interestingly, the presence of CD45.2 *Chrebp*$^{-/-}$ BM, but not of CD45.2 WT BM, increased the number of CD45.1 WT peripheral monocytes, suggesting that monocyte mobilization in mice that had received *Chrebp*$^{-/-}$ BM was mediated by circulating factors (Figure 6F). Thus, the monocytosis in mice that had received *Chrebp*$^{-/-}$ BM was most likely secondary to the

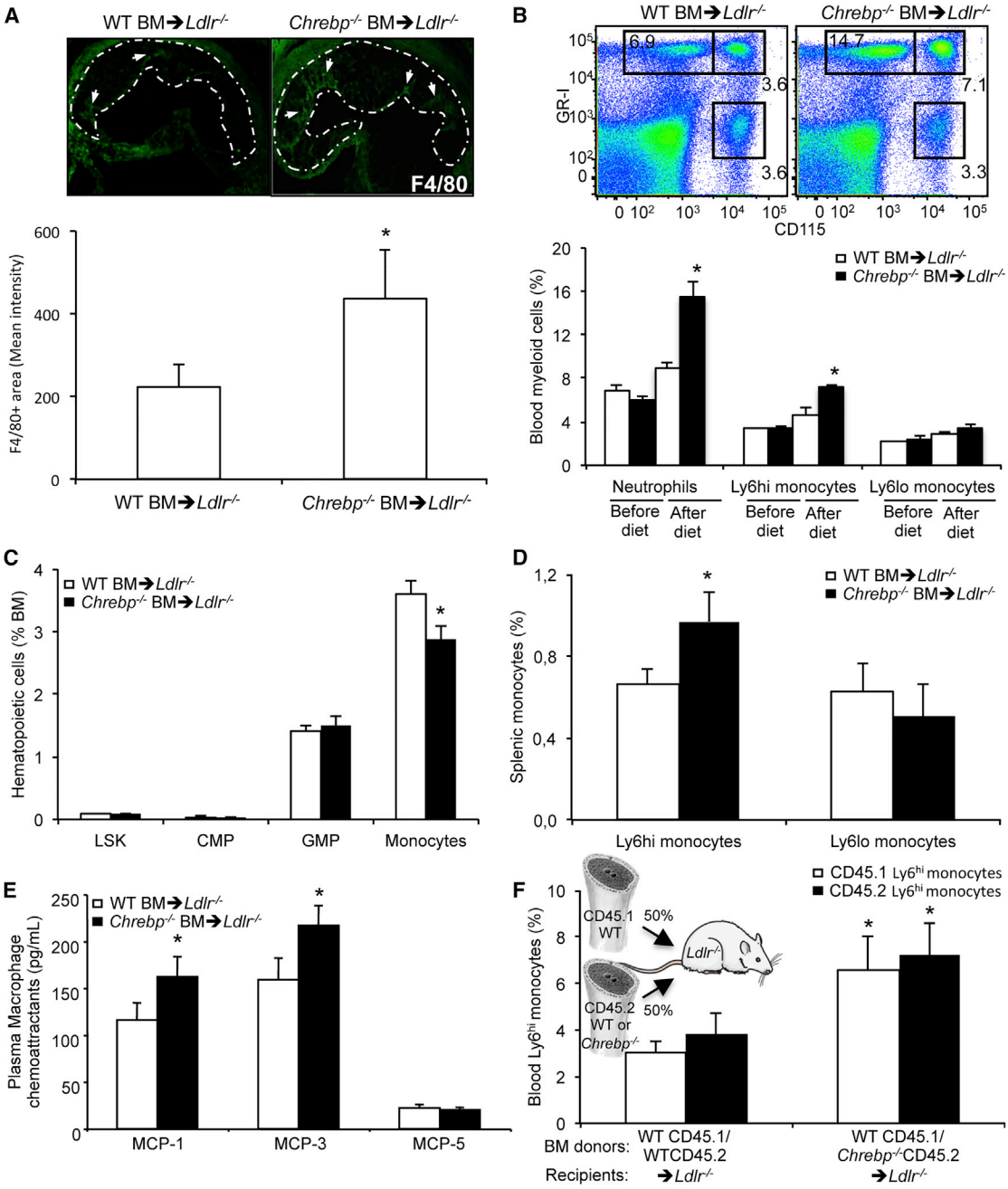

Figure 6. Increased Lesional Macrophages and Inflammatory Monocytes in Mice Transplanted with *Chrebp*$^{-/-}$ BM

(A) Representative pictures and quantification of F4/80+ macrophages in the proximal aorta (magnification ×100) of *Ldlr*$^{-/-}$ mice transplanted with WT or *Chrebp*$^{-/-}$ BM (n = 10).

(B) Representative FACS plots and quantification of peripheral blood myeloid cells.

(C–E) Quantification of BM HSPCs and monocytes (C), splenic monocytes (D), and plasma MCP-1, 3, and 5 levels (E) in these mice.

(F) Competitive BM transplantation of WT CD45.1^{+} BM equally mixed with either CD45.2^{+} WT BM or CD45.2^{+} *Chrebp*$^{-/-}$ BM and transplanted into *Ldlr*$^{-/-}$ recipient mice fed for 11 weeks on an HFD (n = 8). Circulating Ly6^{hi} monocytes were analyzed.

Values are mean ± SEM. *p < 0.05 compared to control.

increased plaque burden and associated systemic inflammation. Future studies using specific knockout of ChREBP in macrophages may help to decipher whether these cells are responsible for the MCP-1 and MCP-3-dependent monocytosis.

Increased Plaque Complexity in *Ldlr*$^{-/-}$ Mice Transplanted with *Chrebp*$^{-/-}$ BM

Histological characterization of atherosclerotic lesions revealed increased plaque complexity in mice that had received *Chrebp*$^{-/-}$

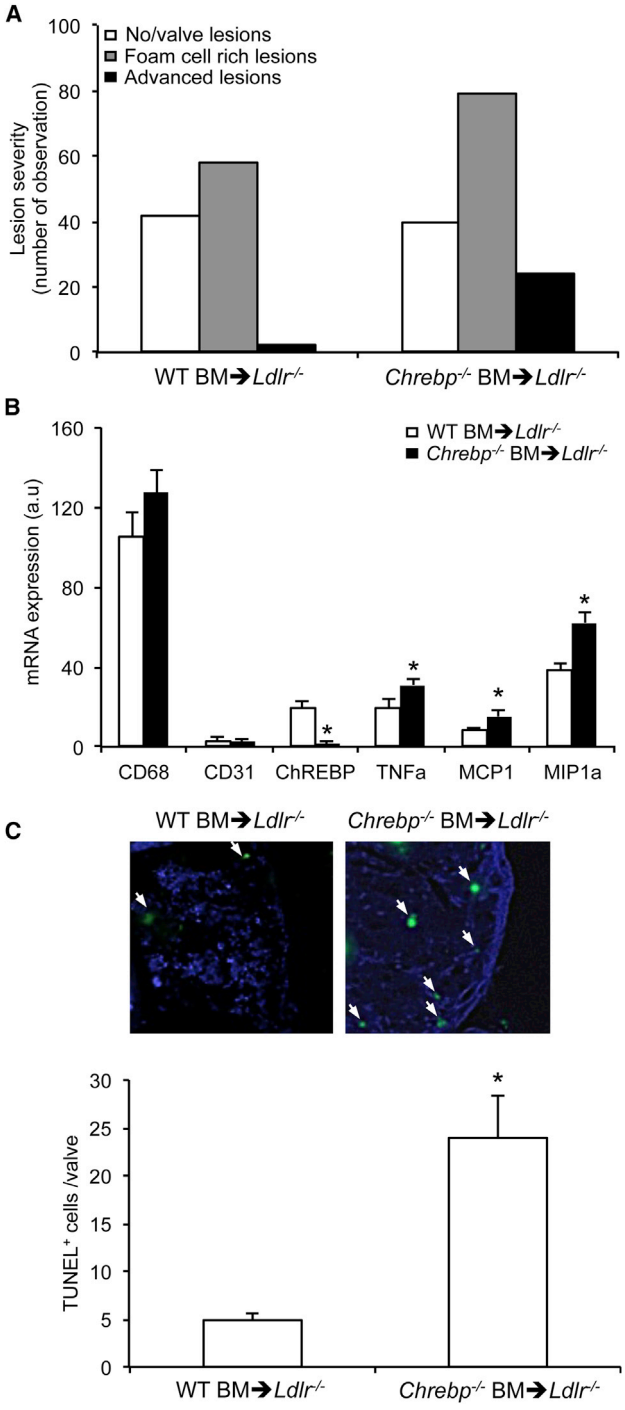

Figure 7. Increased Atherosclerotic Plaque Complexity in Mice Transplanted with *Chrebp*$^{-/-}$ BM

(A) Atherosclerotic lesion severity in the aortic root of HFD-fed *Ldlr*$^{-/-}$ recipient mice transplanted with WT or *Chrebp*$^{-/-}$ BM (n = 10).

(B) mRNA expression in lesional macrophages isolated by laser microcapture in these mice.

(C) Representative micrographs and quantification of TUNEL-positive signal (green; arrows) in nuclei (blue) of aortic root lesions from these mice (magnification ×500).

Results are mean ± SEM. *p < 0.05 compared to control.

BM, typified by a slight decrease in sections containing no lesions or valve lesions and a greater proportion of sections containing foam cell rich lesions and sections containing advanced, complex lesions characterized by compromised integrity of the media, necrotic core formation, and cholesterol clefts (expressed as the number of observations) (Figure 7A). Furthermore, *Chrebp*$^{-/-}$ lesional macrophages isolated by laser capture microscopy (LCM), which expressed CD68, but not the endothelial marker CD31, showed increased mRNA expression of inflammatory cytokines such as TNF-α, MCP-1, and MIP1α (Figure 7B). A trend toward reduced Arg1 and Mrc1 mRNA expression was also observed (data not shown). More strikingly, TUNEL staining revealed five times more apoptotic cells in mice receiving *Chrebp*$^{-/-}$ BM (Figure 7C), reflecting the pro-survival role of ChREBP in maintaining macrophage redox status. This correlated with an increased necrotic area in these mice (1,819 ± 284 versus 3,665 ± 466 μm^2/section in *Ldlr*$^{-/-}$ mice receiving WT or *Chrebp*$^{-/-}$ BM, respectively). Together, these data suggest that ChREBP-dependent metabolic reprogramming of lesional macrophages controls atherosclerosis plaque complexity.

DISCUSSION

Atherosclerotic plaques that cause clinical events, so-called vulnerable plaques, have a high macrophage content (Libby et al., 1996; Moore and Tabas, 2011) that correlates with enhanced ^{18}FDG incorporation visualized by PET-CT imaging (Rogers and Tawakol, 2011; Garcia-Garcia et al., 2014). However, the molecular mechanisms that link glucose utilization to inflammation in macrophages are poorly understood in the context of atherosclerosis. The present study reveals that ChREBP, a glucose sensor transcription factor, is expressed by macrophages and protects against macrophage inflammatory responses and apoptosis induced by pro-atherogenic stressors. Notably, our mechanistic studies have demonstrated that macrophages lacking ChREBP show a dramatic decrease in cellular glutathione content due to the loss of reducing energy supplied through the production of NADPH. This leads to increased ROS production and sustained NF-κB activation in response to LPS in macrophages after ChREBP knockdown, driving local and systemic inflammatory responses. Moreover, in response to oxidative stress-induced apoptosis, macrophages in which ChREBP was silenced were more prone to caspase dependent death, likely explaining the enhanced necrotic core formation in plaques of mice transplanted with *Chrebp*$^{-/-}$ BM. Together, our data establish a critical role for ChREBP in preventing macrophage inflammation and apoptosis in atherosclerosis and demonstrate the importance of immune metabolic flux in chronic inflammatory diseases.

When we initiated the present study, we hypothesized that ChREBP could be a sensor of the high glycolytic rate of inflammatory macrophages (Fukuzumi et al., 1996; Gamelli et al., 1996; Gautier et al., 2013; Nishizawa et al., 2014). This hypothesis was driven by observations showing that ChREBP can be regulated by glucose-derived metabolites in hepatocytes and the fact that liver pyruvate kinase (LPK) is a ChREBP target gene (Filhoulaud et al., 2013). Nevertheless, we first observed that ChREBP was downregulated upon LPS treatment. Basal

and LPS-stimulated ChREBP knockdown macrophages also exhibited higher glycolytic metabolites and enhanced expression of glycolytic enzymes such as Hk2 and PKM2. This suggested that macrophage PKM2, in contrast to hepatic LPK, was not a transcriptional target of ChREBP, most likely because neoglucogenesis is not present in macrophages and these cells do not require fine-tuning of phosphoenolpyruvate (PEP) conversion into pyruvate to avoid its recycling back to PEP for neoglucogenesis (Filhoulaud et al., 2013). The absence of such retro-control in macrophages could also explain the lower expression of ChREBP in these cells compared to hepatocytes. Interestingly, ChREBP is a regulator of malic enzyme (ME)-dependent pyruvate cycling in hepatocytes (Ma et al., 2006; Burgess et al., 2008) that reroutes TCA intermediates derived from pyruvate back to pyruvate and transfers reducing equivalents from NADH to NADP+ to generate NADPH (Lu et al., 2002). The regulation of this pathway appears to be fully conserved in macrophages, as reduced ME expression and activity paralleled a dramatic accumulation of malate in macrophages after ChREBP silencing and was associated with a reduced NADPH/NADP ratio. Alteration of this pathway could also contribute to the broken Krebs cycle recently observed in LPS-stimulated macrophages that could support the arginosuccinate shunt (Jha et al., 2015). There are two alternative metabolic pathways that could have contributed to the reduced NADPH/NADP ratio in these cells. While the reduction of glucose by AR is observed in humans (Vikramadithyan et al., 2005; Srivastava et al., 2009; Vedantham et al., 2011), we observed a decrease in the PGD-dependent nonoxidative phase of the PPP shunt that generates NADPH in macrophages lacking ChREBP, revealing a mechanism of regulation of NADPH production by ChREBP and illustrating the key role of this transcriptional factor in maintaining the redox status of macrophages.

By being a rheostat for cellular metabolism controlling cellular redox status, ChREBP orchestrates a complex response to external pro-atherogenic stressors that require a high energy demand, efficient anti-oxidant homeostasis, and lipid synthesis. Interestingly, the mechanism underlying the increased LPS-dependent inflammatory responses and LPS- and oxidized-LDL-dependent death in macrophages lacking ChREBP was found to be an amplified burst of oxidative stress secondary to a broken TCA cycle and glutathione depletion, which is known to be regenerated in an NADPH-dependent fashion. At the molecular level, the enhanced NF-κB activity in macrophages with ChREBP silencing could be linked to ROS sensitivity (Morgan and Liu, 2011), and ROS generation could also act as a first "hit" signal, pre-polarizing macrophages prior activation (Jais et al., 2014) or sustaining JNK activation (Kamata et al., 2005; Dhanasekaran and Reddy, 2008), altering the balance of life and death in response to Toll-like receptor signaling in macrophages (Yvan-Charvet et al., 2010a; Moore and Tabas, 2011). Glutathione depletion in macrophages has been previously associated with atherosclerotic lesion formation in the setting of AR overexpression (Vikramadithyan et al., 2005; Srivastava et al., 2009; Vedantham et al., 2011). We now show that a similar mechanism can be controlled by ChREBP-dependent NADPH-glutathione regulation. Another interesting observation was that ChREBP controls autophagy-dependent macrophage M2 polarization, which could be the consequence of an altered oxidative metabolism-dependent pre-programming of these cells toward an M2-like phenotype (Jais et al., 2014) or an impaired fatty acid synthesis limiting substrate availability for lysosomal lipolysis (Huang et al., 2014). Future studies should help to clarify this point and determine whether this mechanism contributes to the accelerated atherosclerosis in mice transplanted with *Chrebp*$^{-/-}$ BM (Liao et al., 2012). Together, our studies extend the importance of immune metabolic flux beyond macrophage inflammation in atherosclerosis by proposing that (1) ChREBP could represent a functional metabolic shift between M1 and M2 macrophage polarization in atherosclerosis and (2) ChREBP could play a pivotal pro-survival role in macrophages, with major implications for plaque necrosis and stability (Libby et al., 1996; Moore and Tabas, 2011).

The role of macrophages in controlling hematopoietic and myeloid cell mobilization from the BM to the spleen for extramedullary hematopoiesis has recently emerged. This function represents an important pro-atherogenic mechanism that contributes to the pool of circulating Ly6C^{hi} monocytes that infiltrate atherosclerotic plaques (Tall and Yvan-Charvet, 2015). Interestingly, the increased plaque burden driven by an alteration in macrophage behavior in mice transplanted with *Chrebp*$^{-/-}$ BM was associated with systemic inflammation dominated by an increase in circulating inflammatory Ly6^{hi} monocytes. A competitive BM transplantation experiment suggested that this phenotype was driven by extrinsic factors such as MCP-1 and MCP-3 that were increased in the plasma and atherosclerotic plaques of mice transplanted with *Chrebp*$^{-/-}$ BM. These factors could mediate the emigration of monocytes out of the BM and their recruitment to inflammatory atherosclerotic plaques (Tsou et al., 2007; Tacke et al., 2007; Swirski et al., 2007; Combadière et al., 2008; Westerterp et al., 2013). Thus, this study provides evidence of an additional antiatherogenic effect of ChREBP in macrophages, acting as a positive feedback loop to control monocytosis.

Together, these data demonstrate an unexpected role of ChREBP in preventing macrophage inflammation and apoptosis and indicate that activation of the ChREBP pathway may be a potential therapeutic target to prevent the formation of complex dangerous atheromata. In particular, it would be interesting to determine whether such a therapeutic approach could have additive value in the context of NASH, in which hepatic activation of ChREBP may also protect against insulin resistance (Filhoulaud et al., 2013).

EXPERIMENTAL PROCEDURES

Materials and additional methods are available in Supplemental Experimental Procedures.

Mice

Chrebp$^{-/-}$ mice (B6.129S6-Mlxipltm1Kuy/J) that have been crossed to C57BL/6J for 25 generations were obtained from The Jackson Laboratory. Animal protocols were approved by the Institutional Animal Care and Use Committee of Columbia University or were undertaken according to the Guidelines for Care and Use of Experimental Animals in France. Animals had free access to food and water and were housed in a controlled environment with a 12-hr light-dark cycle and constant temperature (22°C).

BM Transplantation

BM transplantation was performed as previously described (Yvan-Charvet et al., 2010b) using BM from WT and *Chrebp*$^{-/-}$ littermates. Briefly, the atherosclerosis studies were conducted in 10-week-old female *Ldlr*$^{-/-}$ mice fed a Western-type diet (TD88137) from Harlan Teklad for 11 weeks. Mice were allowed to recover for 4 weeks after irradiation and BM transplantation before diet studies were initiated. Body weight was recorded at indicated time points. Mice were euthanized in accordance with the American Veterinary Association Panel of Euthanasia. Spleen and epididymal adipose tissue weights were determined at the time of sacrifice.

Histological Analysis of Proximal Aortas

Mice were sacrificed and heart was harvested. Heart was washed with PBS then fixed with 4% paraformaldehyde. Heart was embedded in paraffin, and 5-μm sections of proximal aortas were performed using a Microm HM340E microtome (Microm Microtech) and stained with H&E. Aortic lesion size of each animal was calculated as the mean of lesion areas in six sections from the same mouse using ImageJ software calibrated with parameters of the Leica DM5500 B (Leica Microsystemes SAS) microscope. Atherosclerotic lesions were expressed in μm^2 per section.

Macrophages Harvesting and Culture

WT mice were injected intraperitoneally with 3% thioglycolate to recruit macrophages as previously described (Gautier et al., 2013). Briefly, after 3 days, mice were sacrificed and peritoneal macrophages were harvested by a PBS (Life Technologies) wash of the intraperitoneal cavity. Cells were filtered on a 42-μM cell strainer (VWR). Macrophages were cultured in DMEM 10% fetal bovine serum 1% penicillin/streptomycin (Life Technologies).

Statistical Analysis

Data are shown as mean ± SEM. Statistical significance was performed using Prism t test or ANOVA were performed according to the dataset. Results were considered as statistically significant when $p < 0.05$.

SUPPLEMENTAL INFORMATION

Supplemental information includes Supplemental Experimental Procedures, seven figures, and two tables and can be found with this article online at http://dx.doi.org/10.1016/j.celrep.2015.08.068.

ACKNOWLEDGMENTS

We thank Dr. Fréderic Labret for assistance with flow cytometry. This work was supported by grants to L.Y.-C. from INSERM ATIP-AVENIR, the Fondation de France (201300038585), and Agence Nationale de la Recherche (ANR). The authors had full access to and take responsibility for the integrity of the data. All authors have read and agree to the manuscript as written.

Received: November 21, 2014
Revised: July 20, 2015
Accepted: August 23, 2015
Published: September 24, 2015

REFERENCES

Burgess, S.C., Iizuka, K., Jeoung, N.H., Harris, R.A., Kashiwaya, Y., Veech, R.L., Kitazume, T., and Uyeda, K. (2008). Carbohydrate-response element-binding protein deletion alters substrate utilization producing an energy-deficient liver. J. Biol. Chem. *283*, 1670–1678.

Cha, J.Y., and Repa, J.J. (2007). The liver X receptor (LXR) and hepatic lipogenesis. The carbohydrate-response element-binding protein is a target gene of LXR. J. Biol. Chem. *282*, 743–751.

Chinetti-Gbaguidi, G., and Staels, B. (2011). Macrophage polarization in metabolic disorders: functions and regulation. Curr. Opin. Lipidol. *22*, 365–372.

Coller, B.S. (2005). Leukocytosis and ischemic vascular disease morbidity and mortality: is it time to intervene? Arterioscler. Thromb. Vasc. Biol. *25*, 658–670.

Combadière, C., Potteaux, S., Rodero, M., Simon, T., Pezard, A., Esposito, B., Merval, R., Proudfoot, A., Tedgui, A., and Mallat, Z. (2008). Combined inhibition of CCL2, CX3CR1, and CCR5 abrogates Ly6C(hi) and Ly6C(lo) monocytosis and almost abolishes atherosclerosis in hypercholesterolemic mice. Circulation *117*, 1649–1657.

Denechaud, P.D., Bossard, P., Lobaccaro, J.M., Millatt, L., Staels, B., Girard, J., and Postic, C. (2008). ChREBP, but not LXRs, is required for the induction of glucose-regulated genes in mouse liver. J. Clin. Invest. *118*, 956–964.

Dentin, R., Tomas-Cobos, L., Foufelle, F., Leopold, J., Girard, J., Postic, C., and Ferré, P. (2012). Glucose 6-phosphate, rather than xylulose 5-phosphate, is required for the activation of ChREBP in response to glucose in the liver. J. Hepatol. *56*, 199–209.

Dhanasekaran, D.N., and Reddy, E.P. (2008). JNK signaling in apoptosis. Oncogene *27*, 6245–6251.

Filhoulaud, G., Guilmeau, S., Dentin, R., Girard, J., and Postic, C. (2013). Novel insights into ChREBP regulation and function. Trends Endocrinol. Metab. *24*, 257–268.

Fukuzumi, M., Shinomiya, H., Shimizu, Y., Ohishi, K., and Utsumi, S. (1996). Endotoxin-induced enhancement of glucose influx into murine peritoneal macrophages via GLUT1. Infect. Immun. *64*, 108–112.

Gamelli, R.L., Liu, H., He, L.K., and Hofmann, C.A. (1996). Augmentations of glucose uptake and glucose transporter-1 in macrophages following thermal injury and sepsis in mice. J. Leukoc. Biol. *59*, 639–647.

Garcia-Garcia, H.M., Jang, I.-K., Serruys, P.W., Kovacic, J.C., Narula, J., and Fayad, Z.A. (2014). Imaging plaques to predict and better manage patients with acute coronary events. Circ. Res. *114*, 1904–1917.

Gautier, E.L., Westerterp, M., Bhagwat, N., Cremers, S., Shih, A., Abdel-Wahab, O., Lütjohann, D., Randolph, G.J., Levine, R.L., Tall, A.R., and Yvan-Charvet, L. (2013). HDL and Glut1 inhibition reverse a hypermetabolic state in mouse models of myeloproliferative disorders. J. Exp. Med. *210*, 339–353.

Hansson, G.K., Robertson, A.K.L., and Söderberg-Nauclér, C. (2006). Inflammation and atherosclerosis. Annu. Rev. Pathol. *1*, 297–329.

Haschemi, A., Kosma, P., Gille, L., Evans, C.R., Burant, C.F., Starkl, P., Knapp, B., Haas, R., Schmid, J.A., Jandl, C., et al. (2012). The sedoheptulose kinase CARKL directs macrophage polarization through control of glucose metabolism. Cell Metab. *15*, 813–826.

Hasty, A.H., and Yvan-Charvet, L. (2013). Liver X receptor α-dependent iron handling in M2 macrophages: The missing link between cholesterol and intraplaque hemorrhage? Circ. Res. *113*, 1182–1185.

Huang, S.C.C., Everts, B., Ivanova, Y., O'Sullivan, D., Nascimento, M., Smith, A.M., Beatty, W., Love-Gregory, L., Lam, W.Y., O'Neill, C.M., et al. (2014). Cell-intrinsic lysosomal lipolysis is essential for alternative activation of macrophages. Nat. Immunol. *15*, 846–855.

Jais, A., Einwallner, E., Sharif, O., Gossens, K., Lu, T.T., Soyal, S.M., Medgyesi, D., Neureiter, D., Paier-Pourani, J., Dalgaard, K., et al. (2014). Heme oxygenase-1 drives metaflammation and insulin resistance in mouse and man. Cell *158*, 25–40.

Jha, A.K., Huang, S.C., Sergushichev, A., Lampropoulou, V., Ivanova, Y., Loginicheva, E., Chmielewski, K., Stewart, K.M., Ashall, J., Everts, B., et al. (2015). Network integration of parallel metabolic and transcriptional data reveals metabolic modules that regulate macrophage polarization. Immunity *42*, 419–430.

Kamata, H., Honda, S., Maeda, S., Chang, L., Hirata, H., and Karin, M. (2005). Reactive oxygen species promote TNFalpha-induced death and sustained JNK activation by inhibiting MAP kinase phosphatases. Cell *120*, 649–661.

Kolodgie, F.D., Virmani, R., Burke, A.P., Farb, A., Weber, D.K., Kutys, R., Finn, A.V., and Gold, H.K. (2004). Pathologic assessment of the vulnerable human coronary plaque. Heart *90*, 1385–1391.

Liao, X., Sluimer, J.C., Wang, Y., Subramanian, M., Brown, K., Pattison, J.S., Robbins, J., Martinez, J., and Tabas, I. (2012). Macrophage autophagy plays a protective role in advanced atherosclerosis. Cell Metab. *15*, 545–553.

Libby, P., Geng, Y.J., Aikawa, M., Schoenbeck, U., Mach, F., Clinton, S.K., Sukhova, G.K., and Lee, R.T. (1996). Macrophages and atherosclerotic plaque stability. Curr. Opin. Lipidol. *7*, 330–335.

Lu, D., Mulder, H., Zhao, P., Burgess, S.C., Jensen, M.V., Kamzolova, S., Newgard, C.B., and Sherry, A.D. (2002). 13C NMR isotopomer analysis reveals a connection between pyruvate cycling and glucose-stimulated insulin secretion (GSIS). Proc. Natl. Acad. Sci. USA *99*, 2708–2713.

Ma, L., Robinson, L.N., and Towle, H.C. (2006). ChREBP*Mlx is the principal mediator of glucose-induced gene expression in the liver. J. Biol. Chem. *281*, 28721–28730.

Macintyre, A.N., Gerriets, V.A., Nichols, A.G., Michalek, R.D., Rudolph, M.C., Deoliveira, D., Anderson, S.M., Abel, E.D., Chen, B.J., Hale, L.P., and Rathmell, J.C. (2014). The glucose transporter Glut1 is selectively essential for CD4 T cell activation and effectyor function. Cell Metab. *20*, 61–72.

Moore, K.J., and Tabas, I. (2011). Macrophages in the pathogenesis of atherosclerosis. Cell *145*, 341–355.

Morgan, M.J., and Liu, Z.G. (2011). Crosstalk of reactive oxygen species and NF-κB signaling. Cell Res. *21*, 103–115.

Mosser, D.M., and Edwards, J.P. (2008). Exploring the full spectrum of macrophage activation. Nat. Rev. Immunol. *8*, 958–969.

Nishizawa, T., Kanter, J.E., Kramer, F., Barnhart, S., Shen, X., Vivekanandan-Giri, A., Wall, V.Z., Kowitz, J., Devaraj, S., O'Brien, K.D., et al. (2014). Testing the role of myeloid cell glucose flux in inflammation and atherosclerosis. Cell Rep. *7*, 356–365.

O'Neill, L.A.J., and Hardie, D.G. (2013). Metabolism of inflammation limited by AMPK and pseudo-starvation. Nature *493*, 346–355.

Ouimet, M., Franklin, V., Mak, E., Liao, X., Tabas, I., and Marcel, Y.L. (2011). Autophagy regulates cholesterol efflux from macrophage foam cells via lysosomal acid lipase. Cell Metab. *13*, 655–667.

Pradelli, L.A., Villa, E., Zunino, B., Marchetti, S., and Ricci, J.E. (2014). Glucose metabolism is inhibited by caspases upon the induction of apoptosis. Cell Death Dis. *5*, e1406.

Randolph, G.J. (2014). Mechanisms that regulate macrophage burden in atherosclerosis. Circ. Res. *114*, 1757–1771.

Rogers, I.S., and Tawakol, A. (2011). Imaging of coronary inflammation with FDG-PET: feasibility and clinical hurdles. Curr. Cardiol. Rep. *13*, 138–144.

Ross, R. (1999). Atherosclerosis–an inflammatory disease. N. Engl. J. Med. *340*, 115–126.

Srivastava, S., Vladykovskaya, E., Barski, O.A., Spite, M., Kaiserova, K., Petrash, J.M., Chung, S.S., Hunt, G., Dawn, B., and Bhatnagar, A. (2009). Aldose reductase protects against early atherosclerotic lesion formation in apolipoprotein E-null mice. Circ. Res. *105*, 793–802.

Swirski, F.K., and Nahrendorf, M. (2013). Leukocyte behavior in atherosclerosis, myocardial infarction, and heart failure. Science *339*, 161–166.

Swirski, F.K., Libby, P., Aikawa, E., Alcaide, P., Luscinskas, F.W., Weissleder, R., and Pittet, M.J. (2007). Ly-6Chi monocytes dominate hypercholesterolemia-associated monocytosis and give rise to macrophages in atheromata. J. Clin. Invest. *117*, 195–205.

Tabas, I. (2005). Consequences and therapeutic implications of macrophage apoptosis in atherosclerosis: the importance of lesion stage and phagocytic efficiency. Arterioscler. Thromb. Vasc. Biol. *25*, 2255–2264.

Tacke, F., Alvarez, D., Kaplan, T.J., Jakubzick, C., Spanbroek, R., Llodra, J., Garin, A., Liu, J., Mack, M., van Rooijen, N., et al. (2007). Monocyte subsets differentially employ CCR2, CCR5, and CX3CR1 to accumulate within atherosclerotic plaques. J. Clin. Invest. *117*, 185–194.

Tall, A.R., and Yvan-Charvet, L. (2015). Cholesterol, inflammation and innate immunity. Nat Immunol Rev *15*, 104–116.

Tannahill, G.M., Curtis, A.M., Adamik, J., Palsson-McDermott, E.M., McGettrick, A.F., Goel, G., Frezza, C., Bernard, N.J., Kelly, B., Foley, N.H., et al. (2013). Succinate is an inflammatory signal that induces IL-1β through HIF-1α. Nature *496*, 238–242.

Tsou, C.L., Peters, W., Si, Y., Slaymaker, S., Aslanian, A.M., Weisberg, S.P., Mack, M., and Charo, I.F. (2007). Critical roles for CCR2 and MCP-3 in monocyte mobilization from bone marrow and recruitment to inflammatory sites. J. Clin. Invest. *117*, 902–909.

Van Vré, E.A., Ait-Oufella, H., Tedgui, A., and Mallat, Z. (2012). Apoptotic cell death and efferocytosis in atherosclerosis. Arterioscler. Thromb. Vasc. Biol. *32*, 887–893.

Vats, D., Mukundan, L., Odegaard, J.I., Zhang, L., Smith, K.L., Morel, C.R., Wagner, R.A., Greaves, D.R., Murray, P.J., and Chawla, A. (2006). Oxidative metabolism and PGC-1beta attenuate macrophage-mediated inflammation. Cell Metab. *4*, 13–24.

Vedantham, S., Noh, H., Ananthakrishnan, R., Son, N., Hallam, K., Hu, Y., Yu, S., Shen, X., Rosario, R., Lu, Y., et al. (2011). Human aldose reductase expression accelerates atherosclerosis in diabetic apolipoprotein E-/- mice. Arterioscler. Thromb. Vasc. Biol. *31*, 1805–1813.

Vikramadithyan, R.K., Hu, Y., Noh, H.L., Liang, C.P., Hallam, K., Tall, A.R., Ramasamy, R., and Goldberg, I.J. (2005). Human aldose reductase expression accelerates diabetic atherosclerosis in transgenic mice. J. Clin. Invest. *115*, 2434–2443.

Westerterp, M., Murphy, A.J., Wang, M., Pagler, T.A., Vengrenyuk, Y., Kappus, M.S., Gorman, D.J., Nagareddy, P.R., Zhu, X., Abramowicz, S., et al. (2013). Deficiency of ATP-binding cassette transporters A1 and G1 in macrophages increases inflammation and accelerates atherosclerosis in mice. Circ. Res. *112*, 1456–1465.

Yvan-Charvet, L., Pagler, T.A., Seimon, T.A., Thorp, E., Welch, C.L., Witztum, J.L., Tabas, I., and Tall, A.R. (2010a). ABCA1 and ABCG1 protect against oxidative stress-induced macrophage apoptosis during efferocytosis. Circ. Res. *106*, 1861–1869.

Yvan-Charvet, L., Pagler, T., Gautier, E.L., Avagyan, S., Siry, R.L., Han, S., Welch, C.L., Wang, N., Randolph, G.J., Snoeck, H.W., and Tall, A.R. (2010b). ATP-binding cassette transporters and HDL suppress hematopoietic stem cell proliferation. Science *328*, 1689–1693.

Zernecke, A., and Weber, C. (2014). Chemokines in atherosclerosis: proceedings resumed. Arterioscler. Thromb. Vasc. Biol. *34*, 742–750.